

Article

The Implication of Injection Locations in an Axisymmetric Cavity-Based Scramjet Combustor

Naresh Relangi ¹, Antonella Ingenito ^{1,*} and Suppandipillai Jeyakumar ^{2,*} 

¹ School of Aerospace Engineering, University of Rome “La Sapienza”, 00138 Rome, Italy; relanginaresh1996@gmail.com

² Aeronautical Engineering, Kalasalingam Academy of Research and Education, Krishnankoil 626126, India

* Correspondence: antonella.ingenito@uniroma1.it (A.I.); sjeyakumar1974@gmail.com (S.J.)

Abstract: This paper presents the effect of cavity-based injection in an axisymmetric supersonic combustor using numerical investigation. An axisymmetric cavity-based angled and transverse injections in a circular scramjet combustor are studied. A three-dimensional Reynolds-averaged Navier–Stokes (RANS) equation along with the $k-\omega$ shear-stress transport (SST) turbulence model and species transport equations are considered for the reacting flow studies. The numerical results of the non-reacting flow studies are validated with the available experimental data and are in good agreement with it. The performance of the injection system is analyzed based on the parameters like wall pressures, combustion efficiency, and total pressure loss of the scramjet combustor. The transverse injection upstream of the cavity and at the bottom wall of the cavity in a supersonic flow field creates a strong shock train in the cavity region that enhances complete combustion of hydrogen-air in the cavity region compared to the cavity fore wall injection schemes. Eventually, the shock train in the flow field enhances the total pressure loss across the combustor. However, a marginal variation in the total pressure loss is observed between the injection schemes.

Keywords: scramjet engine; axisymmetric cavity; transverse injection; computational fluid dynamics; combustion efficiency; total pressure loss



Citation: Relangi, N.; Ingenito, A.; Jeyakumar, S. The Implication of Injection Locations in an Axisymmetric Cavity-Based Scramjet Combustor. *Energies* **2021**, *14*, 2626. <https://doi.org/10.3390/en14092626>

Academic Editor: Suhan Park

Received: 28 March 2021

Accepted: 25 April 2021

Published: 4 May 2021

Publisher’s Note: MDPI stays neutral with regard to jurisdictional claims in published maps and institutional affiliations.



Copyright: © 2021 by the authors. Licensee MDPI, Basel, Switzerland. This article is an open access article distributed under the terms and conditions of the Creative Commons Attribution (CC BY) license (<https://creativecommons.org/licenses/by/4.0/>).

1. Introduction

Supersonic air-breathing engines are the future of high-speed transportation vehicles. Recent studies have witnessed significant progress in the research on scramjets since it is the most suitable and promising engine for the air-breathing hypersonic propulsion [1,2]: the greater specific impulse makes the scramjet appealing for civil and military applications [3]. However, the issues employing supersonic combustion are still unsolved: fuel and oxidizer must mix, ignite, and burn in a very short time, i.e., in a reasonable length avoiding strong shocks within the engine [4]. The crucial and complex task in the design of a scramjet is achieving proper and fast fuel–air mixing, good combustion efficiency, and optimum total pressure losses to make the energy provided by the combustor overcome the drag forces experienced at high velocities. An effective fuel/air mixing and combustion are hard to achieve in scramjets since the residence time is of the order of milliseconds. Previous research efforts have mainly concentrated on injection techniques to maximize the mixing characteristics [5,6]. To design an efficient fuel injector, mixing, combustion, as well as total pressure losses, must be investigated: in fact, there is always a trade-off between the penetration of fuel jet and losses in stagnation pressure since high injection angles lead to strong bow shock which enhances vorticity and mixing inside the flow but also strongly affects the total pressure loss. Deep understanding is, therefore, necessary to answer these key issues.

Several injection strategies have come up with a special interest in generating streamlined vorticity. This is achieved by establishing pressure and density gradients, e.g., employing strategic injector design configurations, such as strut, wall, or swept ramp

injectors, transverse, swirl, and cavities [7–10], which allow the baroclinic waves to arise. A common and simple approach is normal injection through a wall orifice. Before the fuel jet, a bow shock arises due to the obstruction of the free stream by the propellant jet. A barrel shock occurs if the jet is under-expanded and will be terminated by a Mach disk. The high pressure of the fuel jet causes an unfavorable pressure gradient to exist within the boundary layer upstream of the injector causing a separation zone upstream of the injector [11–13]: this region helps to stabilize the flame and achieve mixing; however, this is at the cost of significant total pressure loss.

On the other end, the effect of the bow shock could be reduced by lowering the injection angle (30 and 60 rather than 90 degrees) in a supersonic flow, which results in a reduction of total pressure losses. The axial momentum of the jet also helps to maximize the net thrust. Conclusions made by researchers [14,15] in the case of angled injection stated that the auto-ignition and flames stabilization problems in the scramjet engines could be reduced especially below Mach 10. In recent years, cavities in supersonic combustion chambers have been proposed as a new concept to hold and stabilize the flame. Xing et al. [16] examined the impact of cavity stream on the performance of scramjet combustors. Further studies [17–19] showed that using a cavity after the injector significantly improves the combustion efficiency in a supersonic flow. The effect of sub-cavity in a supersonic cavity flow was studied by Panigrahi et al. [20], who noted that the sub-cavity mitigates the shear layer reattachment at the aft wall of the cavity.

Injecting the fuel upstream of the cavity reports better penetration and mixing and distributes the fuel not only into the main stream but also the cavity. Eventually, most of the oxygen is consumed which improves the efficiency of the combustion [21]. The cavity draws the fuel and air into it to improve the mixing by creating recirculation regions and by holding the products of reaction to stabilize the flame. Barnes et al. [22] stated that injection from the cavity floor makes a more uniform mixing than injecting from the front wall, which made an extremely rich fuel mixture inside the cavity, over the upper combustibility constrain. In the study of Lin et al. [23], it is observed that the distribution of the fuel into subsonic regions of the cavity depends on the injector location upstream of the cavity. From the study, Wang et al. [24] stated that the pressure ratio of fuel to the mainstream plays a significant role in the stabilization modes of the flame in a cavity-based combustor with upstream injection.

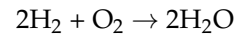
The inclined injection upstream of the cavity reports lower total pressure losses compared to 90 degrees injection and consists of the flame inside of the cavity [25,26]. The mixing of the fuel–air and the efficiency of the combustion is affected by certain factors in case of the injection upstream of the cavity like fuel jet parameters, fuel jet-cavity interaction, and penetration extent of fuel jet [27–29]. Jeong et al. [30] performed three hydrogen injection strategies in a cavity-based scramjet combustor. They reported that upstream injection enhances the fuel diffusion and shorter ignition delay compared to the parallel injection.

From the open literature, it is perceived that injection integrated with cavity encounters the critical characteristics of uniform mixing, flame holding, and stabilization mostly in 2D combustors. The works of literature related to the performance of circular combustor using axisymmetric cavities in a reacting supersonic flow field is scant. This paper investigates the effect of different injection strategies in an axisymmetric cavity-based circular scramjet combustor in a reacting flow field. Three injection schemes are incorporated within the cavity, and the performance is compared with the upstream injection. The performance of the scramjet combustor has been evaluated in terms of wall static pressure, hydrogen and water mass fractions, and combustion efficiency, as well as total pressure loss.

2. Numerical Methods

A 3D RANS equation and $k-\omega$ SST turbulence model [31] have been used to predict the flow field into the combustion chamber employing the commercial code ANSYS Fluent software. A density-based (coupled), implicit, and double-precision scheme has been used

to solve the differential governing equations. Quick convergence is achieved by considering a second-order upwind scheme with an advection upstream splitting method (AUSM) flux vector. Eddy dissipation model has been taken into account for the reactions. The flow is compressible and obeying the laws of an ideal gas. The eddy-dissipation model [32] has been implemented to solve the turbulence–chemistry interaction. A single-step hydrogen–air mechanism has been implemented:

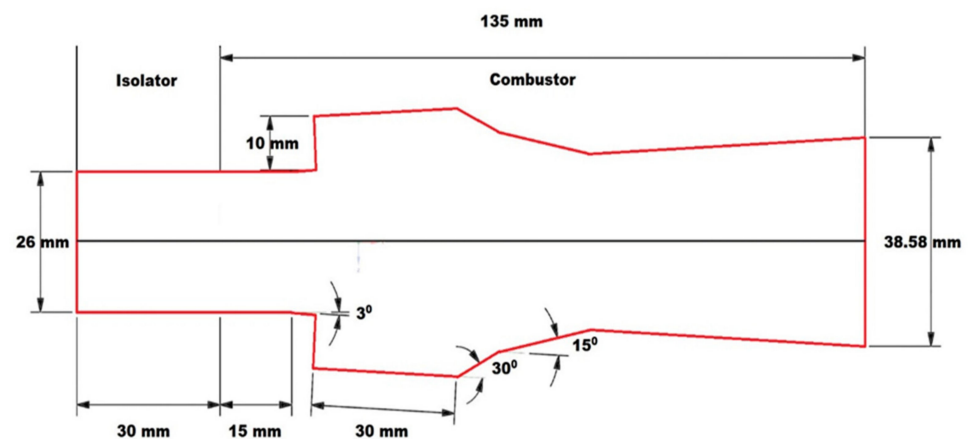


The solutions may be assumed as converged when the residuals have reached their minimum values after declining more than three orders of magnitude, and the deviation between the measured inflow and the outflow mass flow is expected to come down below 0.1%.

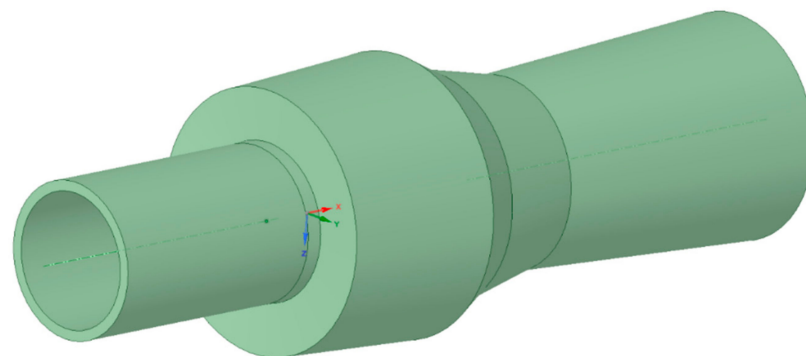
2.1. Geometry Modeling

2.1.1. Computational Domain

The configuration consists of an axisymmetric combustor with a cavity as shown in Figure 1 [33]. The diameter of the inlet is 26 mm, and the whole length of the combustor is 135 mm. Since the ratio between the length and the height of the cavity, L/D , is less than 10, this is called an open cavity. The aft wall of the cavity is divided into two consecutive angles, which are 30° and 15° . Four equi-spaced injectors of 1 mm diameter, placed at four different locations (namely, injection into the cavity at a 45° degree angle, (case 1); injection inside the cavity parallel to the flow, (case 2); transverse injection at the cavity bottom wall (case 3); and injection at a 30° degrees angle upstream of the cavity (case 4)), have been investigated.



(a) The Detailed view of the combustor in 2D



(b) Schematic view of 3D axisymmetric scramjet combustor

Figure 1. The computational domain of the scramjet combustor.

An isolator of length 30 mm and diameter of 26 mm has been placed in front of the combustor to mitigate the effect of the shock train. A divergence of 3 degrees at a distance of 15 mm from the inlet is introduced to avoid thermal choking.

2.1.2. Boundary Conditions

The combustor inlet conditions are those of the experimental test bench in Reference [34]. The inlet conditions of air and hydrogen are reported in the Table 1. No-slip condition is taken into account for the fixed walls.

Table 1. The flow conditions of air and hydrogen.

Variable	Air	H ₂
Ma	1.8	1.0
T (K)	540	300
P (Pascal)	480,000	700,000
t (K)	332	250
P (pascal)	100,000	100,000
ρ (kg/m ³)	1.04	0.097
Y _{O2}	0.232	0
Y _{H2}	0	1
Y _{H2O}	0.032	0

2.1.3. Grid Independence Study

A three-dimensional unstructured grid has been generated using ANSYS Workbench to resolve the flow field in the circular scramjet combustor with an axisymmetric cavity. To optimize the grid resolution and reduce the computational cost and time, three different grid sizes were adopted, namely coarse (140,253), medium (228,607), and fine mesh (330,112). The y^+ value is less than 1.0 for the entire flow field, which corresponds to the 0.001 mm height of the first-row cell. Wall static pressure along the flow direction of the scramjet combustor is considered as a measure for the grid analysis. The results, in Figure 2, show that the deviation between medium and fine grid lies within 1% in terms of wall static pressures. According to the results, it can be stated that medium and fine meshes provide almost identical results compared to the coarse mesh, and the medium mesh is sufficient to carry out the numerical analysis to have a balance between results' accuracy and computational time.

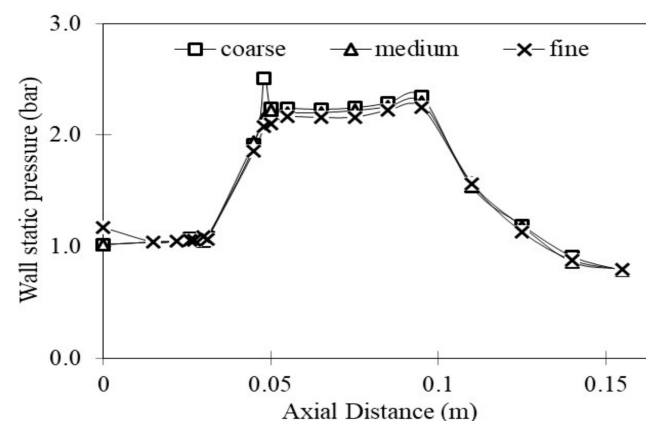


Figure 2. Grid convergence study: static pressure across the bottom wall of the combustor.

3. Results and Discussion

3.1. Validation

Since only non-reacting experiments are performed in Reference [33], the validation of numerical simulations with experimental data has been carried out for similar conditions [35]. The wall static pressures along the flow direction and the momentum

distribution at the exit of the combustor in the radial direction of the flow are compared. A good agreement is observed between numerical and experimental results (Figure 3), and further investigation is performed in the reacting flows with this confidence.

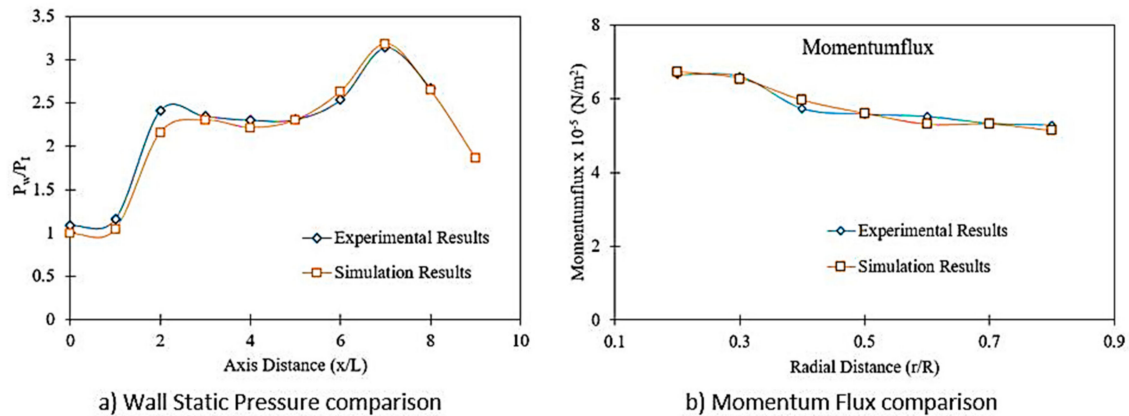


Figure 3. Validation of numerical results with experimental data.

3.2. Flow Field Analysis

The numerical analysis of the scramjet combustor with four different injection angles and locations has been performed. Their respective results have been compared to investigate the implications of these injection strategies in the supersonic flow field and to optimize the injection scheme for the scramjet combustor. Figure 4 shows the Mach number contours for the four injection schemes. In case 1, a 45 degree angled injector is placed at 3 mm on the leading wall of the cavity along the radial direction. The fuel jet enters into the cavity where the flow within the cavity region is subsonic. A 3D Mach disc arises inside the combustor, in the central region, 16 mm downstream the cavity, due to the interaction of the mainstream with fuel jet-induced oblique shocks. A shock train influences the Mach number in the combustor central region, all over the cavity, due to the reflection of strong oblique shocks on the cavity's bottom and top shear layers. For the parallel injection, in case 2, it was observed that flow is supersonic throughout the combustor in the central region and the Mach disc does not arise. This results in low losses in total pressure and a minimum increase (see Figure 7) of the static pressure. In case 3, the transverse injector is located in the cavity at 10 mm downstream of the inlet.

The transverse hydrogen injection leads to the formations of strong oblique shocks and the Mach disc located at 12 mm downstream of the cavity leading edge, between the leading edge and the injectors, i.e., 12 mm upstream of the injection location. The majority of the fuel entered the central region due to normal injection into the cavity. This impact narrows the core flow region all along the cavity. In case 4, a Mach disc arises at 12 mm from the fuel injection, at the beginning of the cavity region.

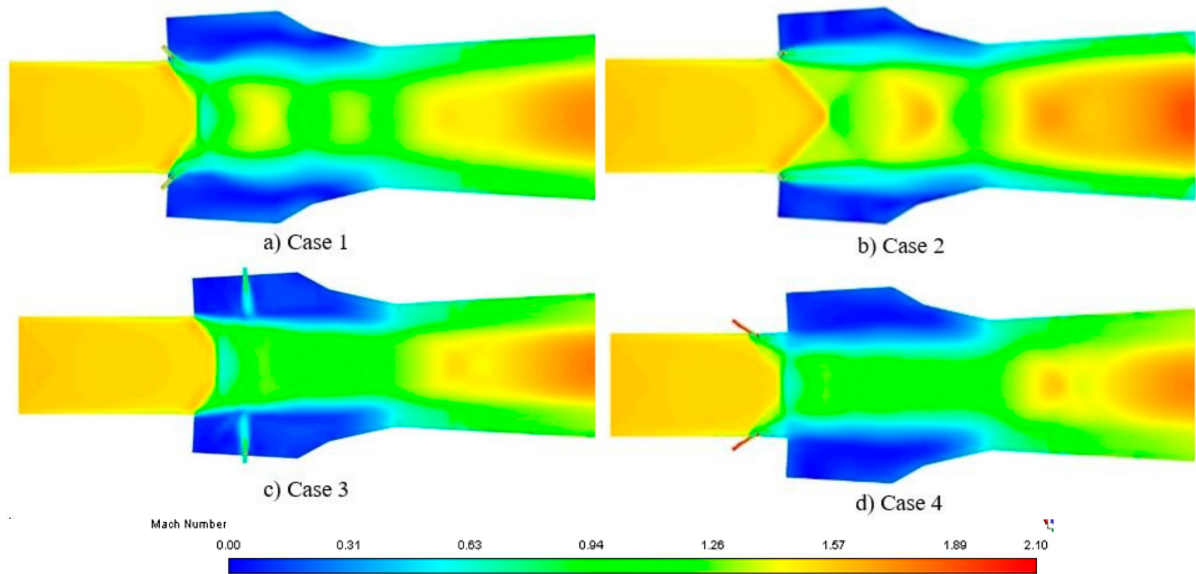


Figure 4. Mach number contour of various injection schemes.

Figure 5 shows the recirculation regions at the various axial planes along the length of the combustor. For case 1, the shear layer separation and reattachment of the flow due to the cavity increase the entrainment of the hydrogen, and air enters into the cavity. The oscillations developed by the cavity enhance the mixing and subsonic regions inside the cavity increases the residence time. In case 2, since the fuel jet moves parallel to the mainstream and the injector is located on the cavity wall, most of the fuel enters into the cavity region (see also Figure 8). In case 3, where the fuel enters in the normal direction to the air, the H_2 jet separates the recirculation zone inside the cavity into two regions, and counter-rotating vortices are formed. These counter-rotating vortices enhance mixing in the cavity region and also the combustion efficiency. Figure 6 shows that the injection of the fuel upstream of the cavity induces the separation of the boundary layer: this plays an important role in generating large recirculation regions within the cavity. The effect of the cavity in cases 3 and 4 is significant in terms of fuel–air mixing and flame-holding compared to other cases.

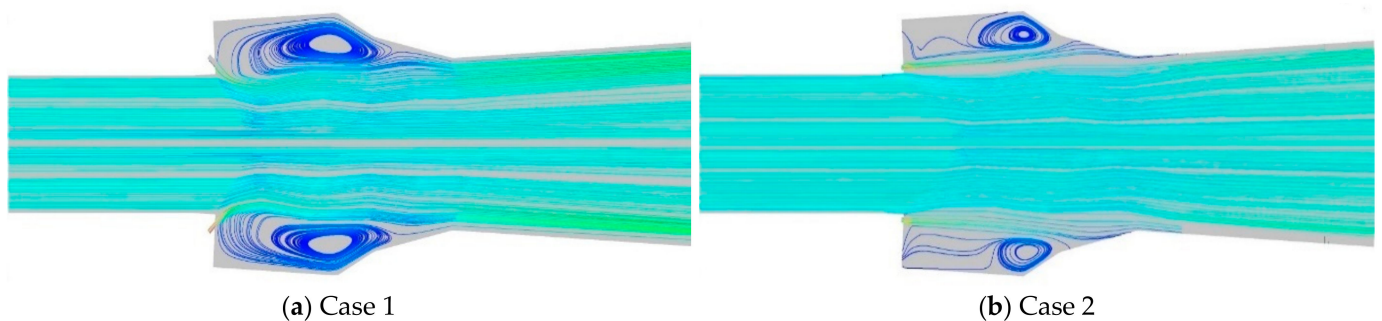


Figure 5. Cont.

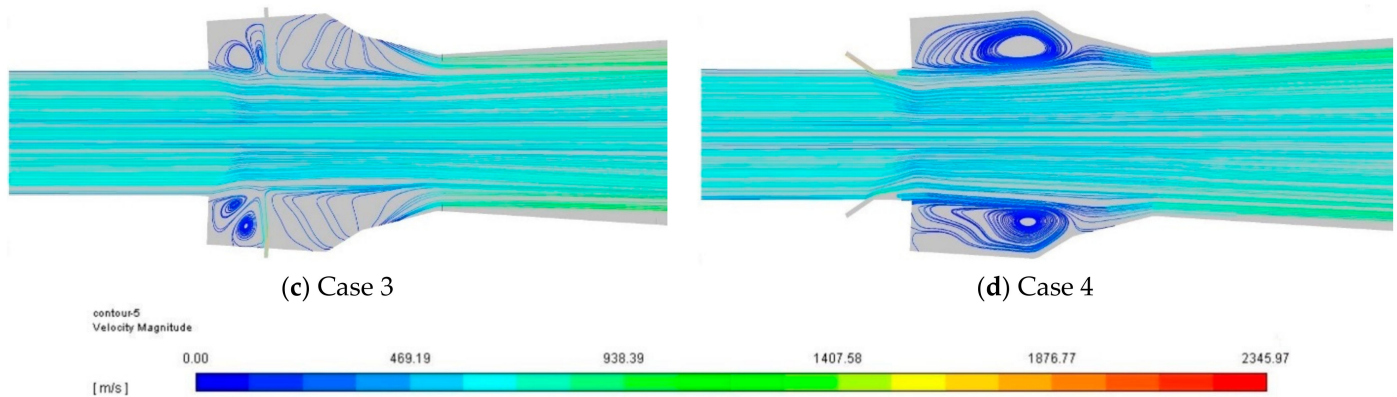


Figure 5. Velocity streamlines of the four injection cases.

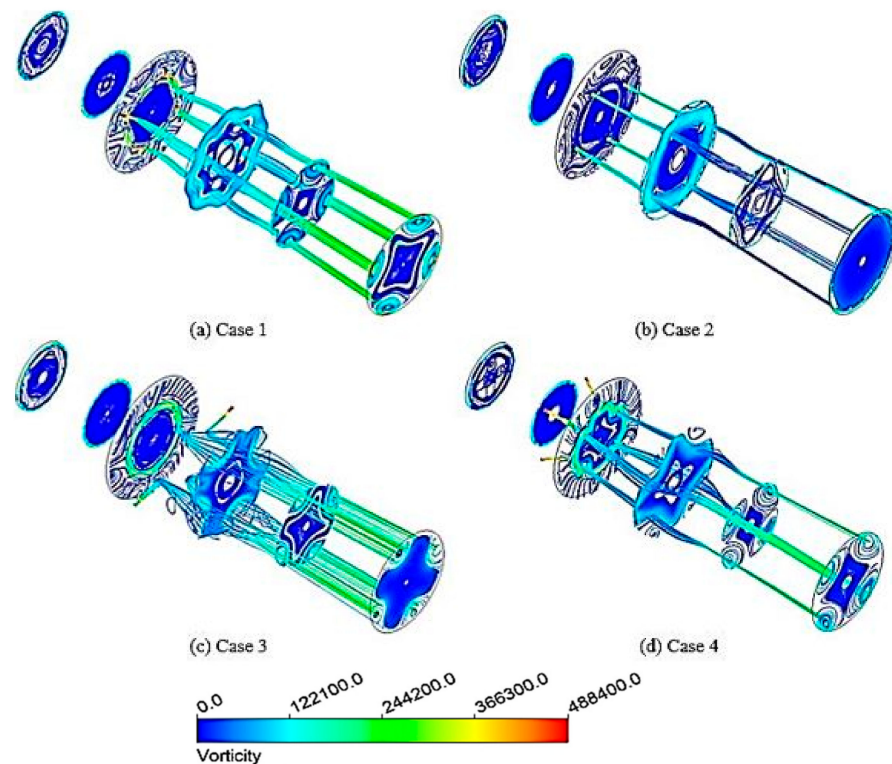


Figure 6. Vorticity contour at the various axial length of the combustor.

3.3. Wall Static Pressure

Figure 7 shows the wall pressure distributions for the different injection strategies. The interaction between shocks, fuel jet, and shear layer led to different peaks of wall static pressures along the combustor for the four cases. It is well known that the shear layer separation and reattachment from the cavity leading and trailing edges of the cavity enhance the wall pressure of the combustor [36]. Among all cases, in case 2, parallel injection reported less wall static pressure throughout the combustor compared to other cases. The parallel injection into the cavity enhances the recirculation resulting in the reduction of wall pressures. The shock train induces the wall pressure rapid changes. In case 3, the transverse fuel from the bottom wall of the cavity generates counter-rotating vortices within the cavity. The interaction of the hydrogen jet with the air stream causes the oblique shock formation and reflection through the top and the bottom shear layer and also the formation of the Mach disc downstream of the cavity leading edge. A peak wall pressure is noted at the trailing wall of the cavity due to strong reattachment of the shear layer, leading to an increase in static pressure. Even though case 1 and case 4 are

both inclined injections, different wall pressure profiles are shown in Figure 6 due to the strength of the recirculation and shear layer reattachment in the cavity region. In case 1, a 3D Mach arises downstream of the cavity leading edge, and the shock train increases the wall static pressure all along the cavity. In case 4, with upstream injection, high wall pressures arise upstream of the cavity due to the strong interaction between the fuel jet, the induced shocks, and the shear layer and the Mach disc located upstream of the cavity. Ultimately, shock train plays a key role in the pressure rise inside the cavity.

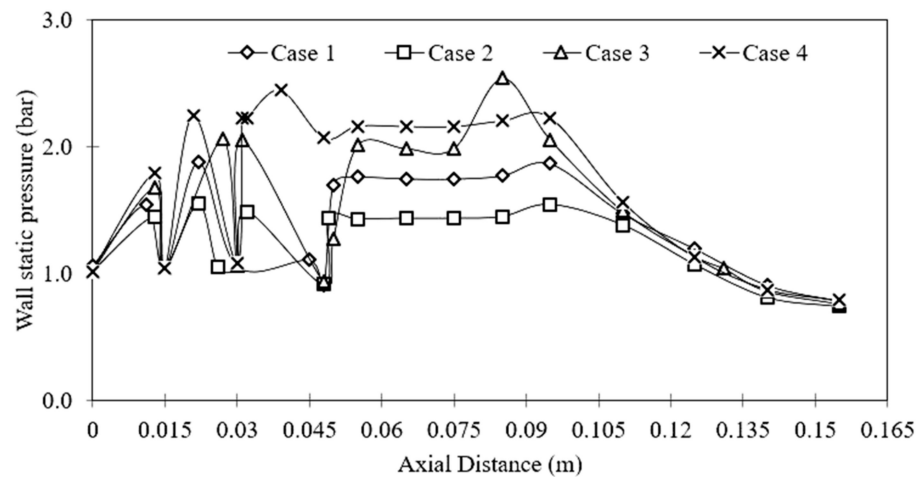


Figure 7. Different combustor geometries static pressure distribution.

3.4. Mass Fraction of H_2 and H_2O

Figures 8 and 9 show the hydrogen and water mass fraction contours, respectively. The jet penetration into the core flow is enhanced by the transverse injection upstream of the cavity. In case 1, the transverse injection at the leading wall of the cavity enhances the hydrogen distribution over the entire cavity region; however, the penetration is not enhanced into the core flow as expected. The fuel jet penetration is low for the parallel injection, i.e., case 2, since the jet moves parallel to the mainstream. Nevertheless, the radicals of reactants have inhabited the entirety of the cavity that could help hold the flame, as observed from the H_2O mass fraction contour.

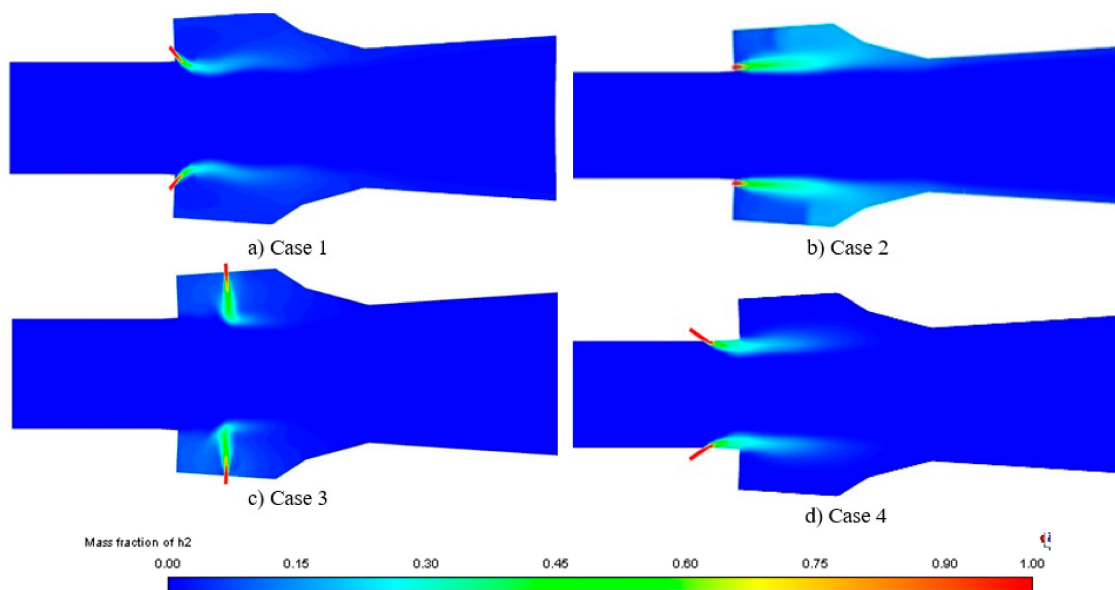


Figure 8. Hydrogen mass fraction contour for the injection schemes.

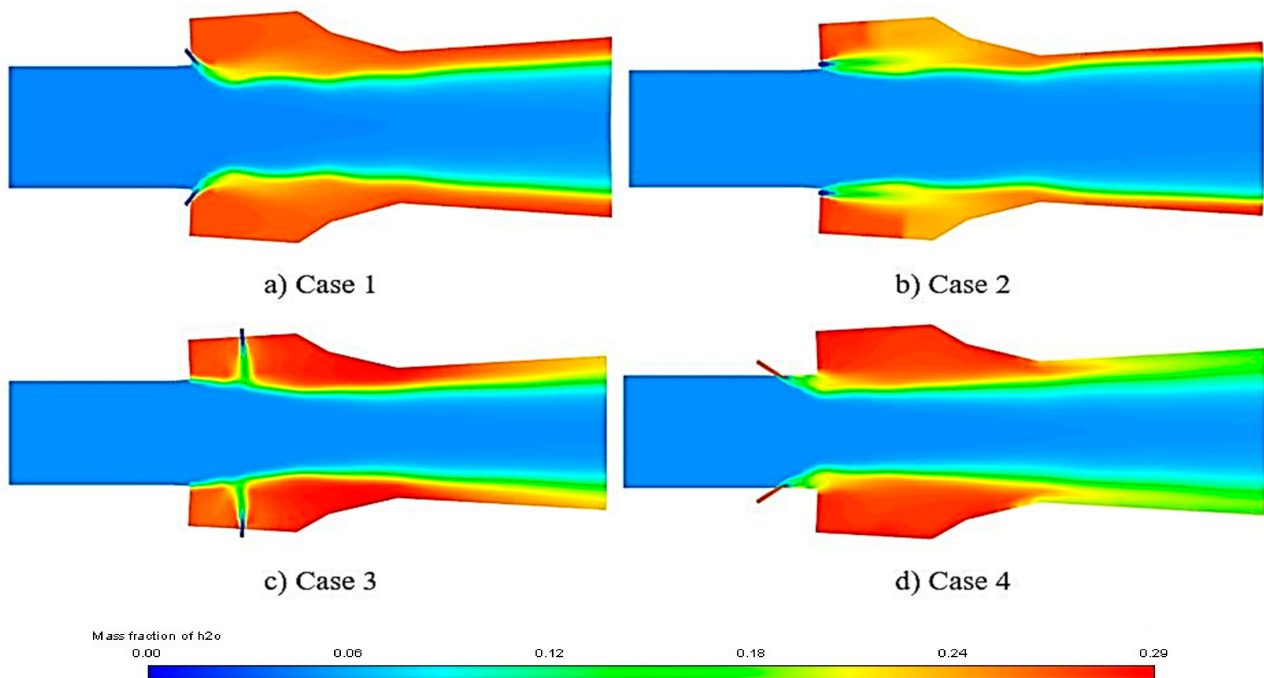


Figure 9. H₂O mass fraction contour for various injection schemes.

In case 3, the normal injection into the cavity disturbs the core flow and the cavity is completely occupied by the products of the reactants. The mixing and combustion of the fuel–air mixture are completed within the cavity region, which is observed from the mass fraction contour. The upstream transverse injection in case 4 the bow shock caused by H₂ injection, interacts with the shear layer as well as the separated boundary layer leading to effective mixing of the fuel into the air throughout the combustor: it is visible from the water mass fraction. The jet penetration into the core flow is enhanced inside the scramjet combustor. The injection of H₂ upstream of the cavity plays a significant role throughout the combustor for the distribution of H₂ and water into the main flow across the overall length of the combustion chamber.

3.5. Temperature Distribution

The static temperature contour for the various injection schemes is shown in Figure 10. The peak temperature distribution is observed for case 4, where maximum temperature distribution is observed in the cavity region, indicating that almost complete combustion is achieved within the cavity regime. Similarly, in case 3, the transverse injection at the bottom wall of the cavity generates counter-rotating vortices within the cavity that enhance mixing and combustion downstream of the injection location in the cavity region. However, in case 1, a uniform heat release is noted from the injection location to the outlet of the combustor. Conversely, the parallel injection in case 1 provides less temperature distribution compared to all other cases indicating that complete combustion could not be attained within the axial length of the combustor.

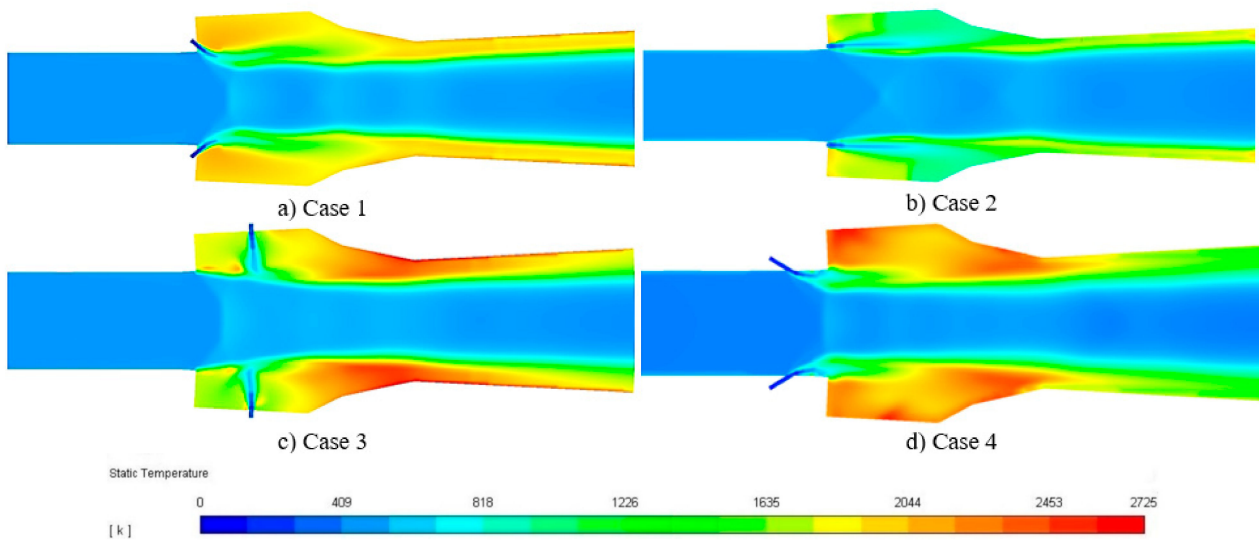


Figure 10. Temperature contour for the various injection schemes.

3.6. Combustion Efficiency

The combustion efficiency through the combustor for various fuel injection strategies is shown in Figure 11. Case 3 and case 4, normal injection from the bottom wall of the cavity and upstream angled injection from the cavity exhibit complete combustion nearly at a distance of 110 mm. In these cases, 100% combustion is achieved. However, an inclined injection into the cavity (case 1) provides nearly 90% combustion efficiency over the entire length of the combustor. However in case 4, the parallel injection into the cavity was not able to burn the fuel completely within the combustor length and recorded 80% combustion efficiency.

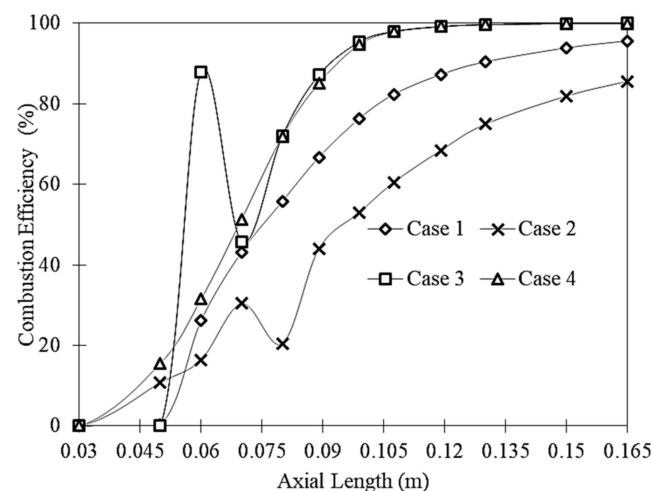


Figure 11. Combustion efficiency across the axial lengths of the combustor for different injection schemes.

3.7. Total Pressure Loss

The total pressure loss across the various axial lengths of the combustor for different injection schemes is shown in Figure 12. The parallel injection from the cavity fore wall in case 2 provides less total pressure loss than other injection cases. This is due to the less interaction of the fuel jet with the core flow in the cavity region. The inclined injection from the fore wall of the cavity provides a much stronger impact on the core flow resulting in an increase in the total pressure loss. The transverse injection from the cavity bottom wall in case 3 provides active counter-rotating vortices in the cavity creates more interaction with

the core flow leads to an enhancement in total pressure loss in the cavity region compared to the other cavity injection. The angled injection upstream of the cavity in case 4 issues higher total pressure loss than injection within the cavity cases. The formation of bow shocks from the injection location interacts with the core flow resulting in the formation of a shock train in the cavity regime, resulting in a reduction of total pressures. However, the total pressure loss across the combustor is almost identical for all the injection cases with a marginal variation of less than 5%.

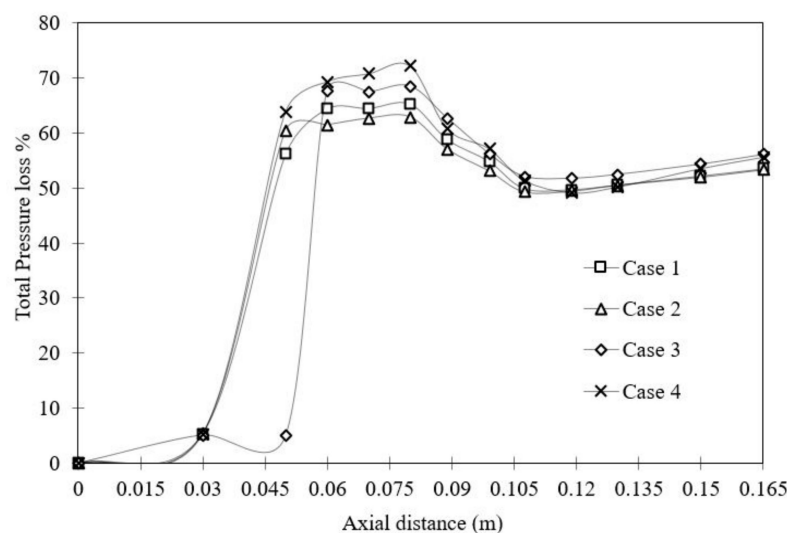


Figure 12. Total pressure loss across the combustor.

4. Conclusions

The computational studies on various injection schemes in an axisymmetric cavity-based scramjet are analyzed using the commercial code ANSYS Fluent software. A three-dimensional RANS equation along with $k-\omega$ SST turbulence model and species transport equations are used to analyze the performance of the injection strategies in the scramjet combustor. The numerical results are validated with the experimental data of the non-reacting flow studies. The key parameters are wall static pressure distribution, combustion efficiency, and total pressure loss across the combustor. The major conclusion of the study are:

- The angled transverse injection upstream of the cavity provides a higher wall pressure profile in the cavity region, indicating that the shock waves generated from the injection location interact with the core flow to create a shock train in the cavity region which creates a compressive zone compared to other cases. The transverse injection at the bottom wall of the cavity provides higher wall pressures in the cavity region compared to the fore wall injection schemes.
- The temperature contour reveals that the upstream and bottom wall injections of the cavity provide higher temperature distribution within the entire cavity, indicating that complete combustion of the hydrogen-air mixture is achieved compared to the injection at the fore wall of the cavity.
- The almost complete combustion is achieved within an axial distance of approximately 110 mm from the combustor inlet by the upstream and bottom wall injection of the cavity.
- The total pressure loss across the combustor is almost identical for all the injection schemes within a marginal variation of less than 5%. From the above observations, the upstream angled injection and bottom wall injection of the cavity provide an enhancement in combustion and flame-holding capabilities with optimum total pressure loss compared to the other injection schemes. These results would be an encouraging pointer for the circular scramjets of hypersonic propulsion applications. The

performances of the injection schemes under varying injection pressures and fuel equivalence ratios are considered for future studies.

Author Contributions: All the authors have contributed equally to this paper. All authors have read and agreed to the published version of the manuscript.

Funding: This research received no external funding.

Institutional Review Board Statement: Not Applicable.

Informed Consent Statement: Not Applicable.

Data Availability Statement: Not Applicable.

Conflicts of Interest: The authors declare no conflict of interest.

Nomenclature

Ma	Mach number
ρ	Density (kg/m^3)
p	Static pressure (Pascal)
P	Total pressure (Pascal)
t	Static temperature (K)
T	Total temperature (K)
k	turbulence kinetic energy
ω	specific dissipation rate
Y_{H_2}	Mass fraction of hydrogen
Y_{O_2}	Mass fraction of oxygen
$Y_{\text{H}_2\text{O}}$	Mass fraction of water

References

- Chang, J.; Zhang, J.; Bao, W.; Yu, D. Research progress on strut-equipped supersonic combustors for scramjet application. *Prog. Aerosp. Sci.* **2018**, *103*, 1–30. [\[CrossRef\]](#)
- Li, L.q.; Huang, W.; Yan, L.; Li, S.b. Parametric effect on the mixing of the combination of a hydrogen porthole with an air porthole in transverse gaseous injection flow fields. *Acta Astronaut.* **2017**, *139*, 435–448. [\[CrossRef\]](#)
- Liu, Q.; Baccarella, D.; Hammack, S.; Lee, T.; Carter, C.D.; Do, H. Influences of freestream turbulence on flame dynamics in a supersonic combustor. *AIAA J.* **2017**, *55*, 913–918. [\[CrossRef\]](#)
- Richard, J.W.; MacKay, J.S. *An Analysis of Ramjet Engines Using Supersonic Combustion*; National Advisory Committee for Aeronautics Collection Tech Note 4386; NACA: Washington, DC, USA, 1952.
- Seleznev, R.K.; Surzhikov, S.T.; Shang, J.S. A review of the scramjet experimental data base. *Prog. Aerosp. Sci.* **2019**, *106*, 43–70. [\[CrossRef\]](#)
- Ren, Z.; Wang, B.; Xiang, G.; Zhao, D.; Zheng, L. Supersonic spray combustion subject to scramjets: Progress and challenges. *Prog. Aerosp. Sci.* **2019**, *105*, 40–59. [\[CrossRef\]](#)
- Athithan, A.A.; Jeyakumar, S.; Sczygiol, N.; Urbanski, M. The Combustion Characteristics of Double Ramps in a Strut-Based Scramjet Combustor. *Energies* **2021**, *14*, 831. [\[CrossRef\]](#)
- Ingenito, A.; Bruno, C. Physics and regimes of supersonic combustion. *AIAA J.* **2010**, *48*, 515–525. [\[CrossRef\]](#)
- Ingenito, A.; Bruno, C. Mixing and combustion in supersonic reactive flows. In Proceedings of the 44th AIAA/ASME/SAE/ASEE Joint Propulsion Conference and Exhibit, Hartford, CT, USA, 21–23 July 2008. AIAA Paper: 2008-4574.
- Ingenito, A.; De Flora, M.G.; Bruno, C.; Giacomazzi, E.; Steelant, J. A Novel Model of Turbulent Supersonic Combustion: Development and Validation. In Proceedings of the 42nd AIAA/ASME/SAE/ASEE Joint Propulsion Conference and Exhibit, Sacramento, CA, USA, 9–12 July 2006; pp. 423–436.
- Gruber, M.R.; Nejad, A.S.; Chen, T.H.; Dutton, J.C. Mixing and penetration studies of sonic jets in a Mach 2 freestream. *J. Propuls. Power* **1995**, *11*, 315–323. [\[CrossRef\]](#)
- Seiner, J.M.; Dash, S.M.; Kenzakowski, D.C. Historical survey on enhanced mixing in scramjet engines. *J. Propuls. Power* **2001**, *17*, 1273–1286. [\[CrossRef\]](#)
- Ogawa, H. Mixing Characteristics of Inclined Fuel Injection via Various Geometries for Upstream-Fuel-Injected Scramjets. *J. Propuls. Power* **2015**, *31*, 1551–1566. [\[CrossRef\]](#)
- Ben Yaker, A.; Hanson, R.K. Experimental Investigation of Flame-Holding Capability of Hydrogen Transverse Jet in Supersonic Cross Flow. *Symp. Int. Comb.* **1998**, *27*, 2173–2180. [\[CrossRef\]](#)
- Ben-Yakar, A. Experimental Investigation of Mixing and Ignition of Transverse Jets in Supersonic Cross flows. Ph.D. Thesis, Stanford University, Stanford, CA, USA, December 2000.

16. Xing, F.; Zhao, M.M.; Zhang, S. Simulations of a cavity based two-dimensional scramjet model. In Proceedings of the 18th Australas Fluid Mechanics Conference AFMC, Launceston, Australia, 3–7 December 2012.
17. Ortwerth, P.J.; Mathur, A.B.; Vinogradov, V.A.; Grin, V.T.; Goldfeld, M.A.; Starov, A.V. Experimental and numerical investigation of hydrogen and ethylene combustion in a Mach 3-5 channel with a single injector. In Proceedings of the 32nd AIAA/ASME/SAE/ASEE Joint Propulsion Conference Exhibit, Lake Buena Vista, FL, USA, 1–3 July 1996.
18. Owens, M.G.; Tehranian, S.; Segal, C.; Vinogradov, V.A. Flame-Holding Configurations for Kerosene Combustion in a Mach 1.8 Airflow. *J. Propuls. Power* **1998**, *14*, 456–461. [[CrossRef](#)]
19. Vinogradov, V.A.; Kobigsky, S.A.; Petrov, M.D. Experimental Investigation of Kerosene Fuel Combustion in Supersonic Flow. *J. Propuls. Power* **1995**, *11*, 130–134. [[CrossRef](#)]
20. Panigrahi, C.; Vaidyanathan, A.; Nair, M.T. Effects of subcavity in supersonic cavity flow. *Phys. Fluids* **2019**, *31*, 036101. [[CrossRef](#)]
21. Wang, H.; Wang, Z.; Sun, M.; Qin, N. Large eddy simulation of a hydrogen-fueled scramjet combustor with dual cavity. *Acta Astronaut.* **2015**, *108*, 119–128. [[CrossRef](#)]
22. Barnes, F.W.; Tu, Q.; Segal, C. Fuel-air mixing experiments in a directly fueled supersonic cavity flameholder. *J. Propuls. Power* **2016**, *32*, 305–310. [[CrossRef](#)]
23. Lin, K.; Tam, C.; Boxx, I.; Carter, C.; Jackson, K.; Lindsey, M. Flame characteristics and fuel entrainment inside a cavity flame holder in a scramjet combustor. In Proceedings of the 43rd AIAA/ASME/SAE/ASEE Joint Propulsion Conference & Exhibit, Cincinnati, OH, USA, 8–11 July 2007. [[CrossRef](#)]
24. Wang, H.; Wang, Z.; Sun, M.; Qin, N. Combustion characteristics in a supersonic combustor with hydrogen injection upstream of cavity flameholder. *Proc. Combust. Inst.* **2013**, *34*, 2073–2082. [[CrossRef](#)]
25. Gruber, M.R.; Donbar, J.M.; Carter, C.D.; Hsu, K.-Y. Mixing and Combustion Studies Using Cavity-Based Flameholders in a Supersonic Flow. *J. Propuls. Power* **2004**, *20*, 769–778. [[CrossRef](#)]
26. Yu, K.H.; Wilson, K.J.; Schadow, K.C. Effect of Flame-Holding Cavities on Supersonic-Combustion Performance. *J. Propuls. Power* **2001**, *17*, 1287–1295. [[CrossRef](#)]
27. Zhang, J.; Chang, J.; Tian, H.; Li, J.; Bao, W. Flame Interaction Characteristics in Scramjet Combustor Equipped with Strut/Wall Combined Fuel Injectors. *Combust. Sci. Technol.* **2020**, *192*, 1863–1886. [[CrossRef](#)]
28. Kim, C.H.; Jeung, I.S. Forced combustion characteristics related to different injection locations in unheated supersonic flow. *Energies* **2019**, *12*, 1746. [[CrossRef](#)]
29. Zhang, J.; Chang, J.; Ma, J.; Wang, Y.; Bao, W. Investigations on flame liftoff characteristics in liquid-kerosene fueled supersonic combustor equipped with thin strut. *Aerosp. Sci. Technol.* **2019**, *84*, 686–697. [[CrossRef](#)]
30. Jeong, E.; O’Byrne, S.; Jeung, I.S.; Houwing, A.F.P. The effect of fuel injection location on supersonic hydrogen combustion in a cavity-based model scramjet combustor. *Energies* **2020**, *13*, 193. [[CrossRef](#)]
31. Li, L.Q.; Huang, W.; Fang, M.; Shi, Y.L.; Li, Z.H.; Peng, A.P. Investigation on three mixing enhancement strategies in transverse gaseous injection flow fields: A numerical study. *Int. J. Heat Mass Transf.* **2019**, *132*, 484–497. [[CrossRef](#)]
32. Magnussen, B.F.; Hjertager, B.H. On mathematical models of turbulent combustion with special emphasis on soot formation and combustion. *Symp. Combust. Inst.* **1976**, *16*, 719–729. [[CrossRef](#)]
33. Jeyakumar, S.; Assis, S.M.; Jayaraman, K. Experimental study on the characteristics of axisymmetric cavity actuated supersonic flow. *J. Aerosp. Eng.* **2017**, *231*, 2570–2577. [[CrossRef](#)]
34. Assis, S.M.; Suppandipillai, J.; Kandasamy, J. Transverse Injection Experiments within an Axisymmetric Scramjet Combustor. *Int. J. Turbo Jet-Engines* **2019**. [[CrossRef](#)]
35. Relangi, N.; Garimella, D.; Jayaraman, K.; Venkatesan, J.; Jeyakumar, S.; Ingenito, A. Numerical simulations of axisymmetric aft wall angle cavity in supersonic combustion ramjets. In Proceedings of the AIAA Propuls, Energy 2020 Forum, Virtual Event, 24–28 August 2020; pp. 1–15.
36. Ben-Yakar, A.; Hanson, R.K. Cavity Flame-Holders for Ignition and Flame Stabilization in Scramjets: An Overview. *J. Propuls. Power* **2001**, *17*, 869–877. [[CrossRef](#)]